


Cross-Frequency Coupling as a Biomarker for Early Stroke Recovery

Jasper I. Mark, BS^{1,2}, Justin Riddle, PhD³,
Rachana Gangwani, PT, MS^{1,2}, Benjamin Huang, MD, MPH⁴,
Flavio Fröhlich, PhD^{5,6}, and Jessica M. Cassidy, DPT, PT, PhD^{2,*} 

Neurorehabilitation and
Neural Repair
2024, Vol. 38(7) 506–517
© The Author(s) 2024



Article reuse guidelines:
sagepub.com/journals-permissions
DOI: 10.1177/15459683241257523
journals.sagepub.com/home/nnr



Abstract

Background. The application of neuroimaging-based biomarkers in stroke has enriched our understanding of post-stroke recovery mechanisms, including alterations in functional connectivity based on synchronous oscillatory activity across various cortical regions. Phase-amplitude coupling, a type of cross-frequency coupling, may provide additional mechanistic insight. **Objective.** To determine how the phase of prefrontal cortex delta (1-3 Hz) oscillatory activity mediates the amplitude of motor cortex beta (13-20 Hz) oscillations in individual's early post-stroke. **Methods.** Participants admitted to an inpatient rehabilitation facility completed resting and task-based EEG recordings and motor assessments around the time of admission and discharge along with structural neuroimaging. Unimpaired controls completed EEG procedures during a single visit. Mixed-effects linear models were performed to assess within- and between-group differences in delta-beta prefrontomotor coupling. Associations between coupling and motor status and injury were also determined. **Results.** Thirty individuals with stroke and 17 unimpaired controls participated. Coupling was greater during task versus rest conditions for all participants. Though coupling during affected extremity task performance decreased during hospitalization, coupling remained elevated at discharge compared to controls. Greater baseline coupling was associated with better motor status at admission and discharge and positively related to motor recovery. Coupling demonstrated both positive and negative associations with injury involving measures of lesion volume and overlap injury to anterior thalamic radiation, respectively. **Conclusions.** This work highlights the utility of prefrontomotor cross-frequency coupling as a potential motor status and recovery biomarker in stroke. The frequency- and region-specific neurocircuitry featured in this work may also facilitate novel treatment strategies in stroke.

Keywords

stroke, neuroimaging, connectivity, biomarker, rehabilitation

Introduction

The optimization of patient care, which involves the precise tailoring and delivery of treatments and therapies, depends on our understanding of underlying neural mechanisms that promote post-stroke recovery. The application of neuroimaging and neurophysiological measurements in stroke has revealed a vast spectrum of post-stroke alterations in brain structure and function.¹ These brain-based measurements may serve as prognostic indicators, or biomarkers of recovery with the potential to enhance the prediction of post-stroke outcomes and inform treatment strategies.²

Electroencephalography (EEG) affords temporally resolute measurements of neural oscillatory activity.³ In stroke, there have been a number of studies showing associations between region- and frequency-specific oscillatory synchronization and coherence (connectivity) with functional status⁴ and training/rehabilitation-induced changes in functional status.^{5,6} While stroke is a vascular disorder that often leads to impaired brain and body function, this evidence

¹Human Movement Science Curriculum, University of North Carolina at Chapel Hill, Chapel Hill, NC, USA

²Department of Health Sciences, University of North Carolina at Chapel Hill, Chapel Hill, NC, USA

³Department of Psychology, Florida State University, Tallahassee, FL, USA

⁴Department of Radiology, University of North Carolina at Chapel Hill, Chapel Hill, NC, USA

⁵Carolina Center for Neurostimulation, University of North Carolina at Chapel Hill, Chapel Hill, NC, USA

⁶Department of Psychiatry, University of North Carolina at Chapel Hill, Chapel Hill, NC, USA

*This author is a member of the American Society of Neurorehabilitation.

Supplementary material for this article is available on the *Neurorehabilitation & Neural Repair* website along with the online version of this article.

Corresponding Author:

Jessica M. Cassidy, Department of Health Sciences, University of North Carolina at Chapel Hill, 321 South Columbia Street, Chapel Hill, NC 27514, USA.

Email: jcassidy@med.unc.edu

supports the view of stroke as a disease of “circuitopathies” as characterized by disruptions to typical connectivity.⁷

Stroke may also result in altered coupling of oscillatory activity across the frequency domain.⁸ Rather than operating in isolation, network scale activity in the low-frequency range may play a critical role in organizing localized activity in the high-frequency range of distinct cortical areas.⁹ Phase-amplitude coupling (PAC) is a type of cross-frequency coupling whereby the phase of low-frequency oscillatory activity gates the amplitude of higher-frequency oscillations.^{10,11} Recent work by Rustamov et al¹² showed functional motor recovery across 17 individuals with stroke was associated with increased local theta-gamma coupling in bilateral primary motor (M1) regions. Additional research has demonstrated that rhythms associated with motor function (ie, beta) from M1 are regulated by low-frequency rhythms (ie, delta) arising from prefrontal cortex (PFC).^{10,13,14} Delta oscillations from PFC are engaged by a variety of tasks that require higher-order cognitive functions (eg, attention, working memory, and decision-making), which impact motor planning, execution, and coordination.^{10,15} When applied to a clinical population, such as people with depression, a reduction in delta-beta PAC (DB-PAC) was associated with decreased goal-directed behavior.¹³ Because stroke rehabilitation involves goal-mediated behavior to improve capacity across multiple functional domains such as cognition, speech, and motor, these prefrontal-gating disruptions may prove relevant during stroke recovery.^{16,17}

This study builds upon past work highlighting the roles of prefrontomotor connections in people with depression and anxiety^{18,19} along with delta and beta oscillatory activity in stroke recovery.^{5,20,21} Here, we measured prefrontomotor (PFC-M1) DB-PAC using resting- and task-based EEG recordings in individuals early post-stroke and unimpaired controls. We hypothesized that coupling would vary between resting and task conditions due to heightened cognitive and motor control demands of the latter condition. As increased prefrontomotor oscillatory control during task performance with the stroke-affected extremity might represent a compensatory mechanism, we also hypothesized that the magnitude of DB-PAC would decline over time in parallel with post-stroke motor recovery.

Given premotor cortex (PMC) engagement during motor planning and movement preparation and its close anatomical approximation to PFC and M1,²² PMC is a key site for the integration of motor and cognitive function.^{23,24} Non-human primate work have shown ventrorostral PMC involvement in visual and somatosensory information processing for motor control.^{25,26} Work in humans entailing “virtual” lesions to ventral PMC also resulted in impaired grip performance (ie, finger positioning and muscle recruitment).^{27,28} Together, this evidence substantiates PMC

involvement in both visuomotor interactions and movement execution. Additional work that is particularly relevant to our study also suggests the involvement of PMC in precision grip tasks during the estimation of grip magnitude and grip sustainment.^{18,28} We therefore sought to determine the influential role of PMC in prefrontomotor coupling by examining the PFC-PMC-M1 pathway, hypothesizing that prefrontomotor coupling occurs through PMC.

The final objective of this work was to better understand the impact of stroke-related injury on DB-PAC or to what extent does downstream injury impact upstream activity. The cortico-basal ganglia-thalamo-cortical loop (CBGTC loop) plays an instrumental role in motor control and learning.^{19,29,30} The thalamus possesses an expansive network of bidirectional fiber connections with multiple cortical areas, including the PFC via the anterior thalamic radiation (ATR) and M1 via the posterior thalamic radiation.³¹ These thalamocortical pathways enable the thalamus to synchronize activity across distant cortical regions during movement planning and execution.²⁹ Recent work has specifically highlighted the anterior thalamus and its projections through the ATR in mediating beta oscillatory signaling critical for motor sequencing.^{32,33} We therefore expected that stroke-related injury to components comprising the CBGTC loop (basal ganglia and ATR, specifically) would disrupt prefrontomotor DB-PAC.

Methods

Participants

We recruited individuals with a radiologically confirmed stroke (ischemic or hemorrhagic) aged ≥ 18 years that were admitted to an inpatient rehabilitation facility (IRF) from November 2020 to February 2022. Participants completed a total of 2 visits with visit 1 occurring at around the time of IRF admission and visit 2 occurring around the time of IRF discharge. Visits involved a 3-minute resting-state EEG recording, a task-based EEG recording featuring a precision grip activity, and behavioral assessments to evaluate motor impairment (Upper Extremity Fugl-Meyer, UEFM) and motor function (Action Research Arm Test, ARAT). Motor recovery was assessed by computing ARAT and UEFM $\text{Change}_{\text{Realized}}$ during IRF stay by normalizing their change in behavior (Visit 2 – Visit 1) to recovery potential (Max – Visit 1) using the following equation³⁴:

$$\text{Change}_{\text{Realized}} = \frac{\text{Visit 2} - \text{Visit 1}}{\text{Max} - \text{Visit 1}} \quad (1)$$

A control cohort consisting of right-handed adults without a history of stroke were also recruited from the local community. The cohort completed a single baseline visit consisting of resting- and task-based EEG recordings. This study protocol received approval from the University of

North Carolina at Chapel Hill Institutional Review Board. All subjects provided written informed consent. Anonymized data are available and may be accessed through UNC Dataverse at <https://doi.org/10.15139/S3/P9LDFH>.

EEG Acquisition and Processing

Resting-State EEG. Individuals completed a 3-minute resting-state EEG recording with eyes open using a dense-array (256-lead) Hydrocel net (Electrical Geodesics Inc., Eugene, OR). EEG data were collected at a sample rate of 1000Hz using a high input impedance Net Amp 300 amplifier and Net Station 5.4.2 software (Electrical Geodesics Inc.). Consistent with previous work,^{5,20,35} raw EEG data were exported to MATLAB 2017b (MathWorks, Natick, MA) for offline processing in EEGLAB. Data were bandpass filtered between 0.5 and 50Hz, and electrodes overlying the cheek and neck regions were removed leaving 194 electrodes for further analysis. The signal was re-referenced to the average scalp. Following visual inspection, data underwent an infomax components analysis to remove ocular, cardiac, and muscular artifacts.³⁶ An additional round of visual inspection of the data occurred after artifact removal. EEG data from participants with stroke were standardized so that the left hemisphere corresponded to the ipsilesional hemisphere.

Task-Based EEG. Individuals completed a task-based EEG recording with simultaneous electromyography collection. During the recording, participants performed an isometric grip task at 20% of their maximum grip force over 2 blocks of 20 trials with visual feedback provided. Participants were randomized so that approximately half completed the task with their dominant/affected extremity first. EEG data were processed as described above. Task data were analyzed during the middle 3 seconds of the grip trial to capture the sustained isometric contraction.

Regions of Interest. Electrode-based regions of interest were selected in accordance with the international 10 to 20 system.³⁵ Ipsilesional, or left, M1 included C3 and the 6 surrounding electrodes. Contralesional, or right, M1 entailed C4 and the 6 surrounding electrodes. Bilateral PMC represented a 6-electrode cluster located anterior-adjacent to homotopic M1 regions. Previous work has shown bilateral recruitment of PFC for executive control and decision-making.³⁷ This bilateral recruitment may result in signals depicting peak activation along the central midline due to volume conduction.³⁸ Guided by these findings, we chose our PFC region of interest to include bilateral prefrontal regions and midline, which encompassed 23 electrodes surrounding and situated between canonical anterior PFC electrodes Fp1 and Fp2.

A complete list and illustration of electrode-based regions of interest are provided in Supplemental Table 1 and Supplemental Figure 1, respectively.

Phase-Amplitude Coupling

Computation of PAC using preprocessed EEG data occurred in MATLAB. PAC was calculated with respect to bilateral PFC delta (1-3 Hz) phase and beta (13-20Hz) amplitude in electrodes overlying bilateral M1 during rest and contralateral M1 during task performance. This corresponded to electrodes overlying left M1 during task performance with the affected/dominant extremity and electrodes overlying right M1 during task performance with the less-affected/non-dominant extremity. PAC values were calculated according to *mean vector length* as it minimizes potential inflation and/or false presence of coupling.^{11,14,39} First, instantaneous delta phase and beta amplitude were extracted for each trial and then the data were concatenated before a single estimation was calculated. Values were normalized based on a null distribution generated by shifting the amplitude values with a random temporal offset of at least 10% the length of the time series.^{11,14}

Processed data also underwent a cluster analysis to determine the between- and within-group effects of other cortical regions on DB-PAC. PFC delta phase and beta amplitude for individual electrodes across the scalp were computed. A series of *t*-tests were performed between individuals with stroke and healthy controls for each Extremity, Condition, and Time. Given the large number of electrodes involved (194 across the scalp), we applied a Bonferroni correction ($P=.00026$) to correct for multiple comparisons. Electrodes were then clustered into the nearest 10 to 20 positions. The Group and Time interactions for each cluster were computed across each Extremity and Condition.

MRI Acquisition

Participants completed a structural magnetic resonance imaging (MRI) scan on either a 3-Tesla Siemens MAGNETOM TrioTim Syngo or Skyra scanner or a 1.5-Tesla Siemens MAGNETOM Aera scanner during their hospitalization. Imaging included a high-resolution T1-weighted scan using a 3-dimensional magnetization-prepared rapid gradient echo sequence (repetition time=2300ms, echo time=2.91-3.26ms, 160 slices, 1 mm³ isotropic voxel) and a T2-weighted fluid-attenuated inversion recovery scan (repetition time=9000ms, echo time=115ms, 31 slices, voxel size=0.9×0.9×5 mm³). Data were standardized so that the left hemisphere represented the ipsilesional hemisphere.

Stroke-Related Injury

Lesion Volume. Using similar methodology validated in stroke,⁴⁰ lesion masks for each participant were manually defined in MRIcron on T1-weighted slices with further information provided by the T2-fluid-attenuated inversion recovery scans. Lesion masks were reviewed by a neuroradiologist (BH). Lesion volumes were determined from these masks as a measure of global stroke injury. Individuals with direct lesion involvement to the PFC and/or M1 were removed from subsequent PAC correlational analyses.

Lesion Overlap With Subcortical Structures. We also measured lesion overlap injury to basal ganglia and ATR to assess stroke-related injury more specific to PAC. Lesion masks were binarized and spatially transformed to Montreal Neurological Institute standard stereotaxic space. We computed overlap injury as the percentage of lesion-voxel overlap from basal ganglia, ATR, and corticospinal tract (CST) from the Automated Anatomical Labeling and Johns Hopkins University white matter tractography atlases, respectively.^{41,42}

Statistical Analysis

Statistics were performed in JMP Pro17 (SAS, Cary, NC). Statistical tests included a series of mixed-effects linear models to assess PFC-M1 DB-PAC with regards to effects of Group (stroke vs controls), Condition (rest vs task), Extremity (Stroke: affected vs less-affected; Controls: dominant vs non-dominant), and Time (visit 1 vs visit 2). Each participant served as a random intercept to model within-subject correlation. Post-hoc analyses involved pairwise comparisons using Tukey's honestly significant difference with an alpha value of .05 denoting significance. The above models were repeated with PFC delta and M1 beta power for a control analysis. For analyses involving task-based EEG data, affected and less-affected extremity measurements for each participant were included whenever possible. For those unable to perform the task, data from that extremity were not included in the computation of group means for that extremity during the task condition at that visit.

To preliminarily assess the role of PMC in PFC-M1 coupling, we performed a partial correlation (r_{partial}) analysis between PFC-M1, PFC-PMC, and PMC-M1 connections. Lastly, to evaluate associations between coupling with injury (lesion overlap and percent overlap injury) and motor assessments (UEFM, ARAT, and grip strength), we computed correlation coefficients. For both partial correlation and correlation analyses, an alpha value $\leq .05$ was significant.

Results

Participants

We enrolled 30 individuals with stroke (10.4 ± 3.5 days post-stroke; 67.0 ± 9.8 years of age; 14 females) admitted to

an IRF where they received post-stroke care over an average of 14.0 ± 6.2 days. The cohort demonstrated considerable heterogeneity with respect to lesion characteristics and baseline motor impairment (UEFM) and motor function (ARAT) as depicted in Table 1. Of those 30 participants, 20 successfully completed the precision grip task in both extremities (affected: $n=21$; less-affected: $n=28$) at visit 1 around the time of IRF admission. By visit 2, around the time of IRF discharge, 26 participants successfully completed the precision grip task in both extremities (affected: $n=26$; less-affected: $n=29$). During IRF hospitalization, 5 individuals (16.7%) were prescribed baclofen, and 12 individuals (40%) were taking antiseizure and/or antidepressant medication. Seventeen control participants (75.3 ± 13 years of age, 8 females) without stroke were also enrolled.

Elevated PFC-M1 Coupling During Task Performance

The mixed-effects linear model to investigate the effects of Condition and Group on PFC-M1 DB-PAC for visits 1 and 2 revealed a significant Condition effect at both visits (Visit 1: $F_{(1,65.2)}=17.12$, $P<.001$; Visit 2: $F_{(1,71.3)}=19.62$, $P<.001$; Figure 1 and Supplemental Table 2) with post-hoc tests demonstrating greater PFC-M1 DB-PAC during task versus rest (Visit 1: $(t_{(65.2)})=4.14$, $P<.001$; Visit 2: $(t_{(71.3)})=4.43$, $P<.001$). The model also depicted a significant Group effect at visit 1 ($F_{(1,38.4)}=17.01$, $P<.001$; Figure 1 and Supplemental Table 2) with post-hoc testing indicating greater PFC-M1 DB-PAC in individuals with stroke ($(t_{(38.4)})=4.12$, $P<.001$). Group differences were not present at visit 2 ($F_{(1,47.7)}=2.97$, $P=.091$).

We performed a similar model to evaluate the within-stroke-group differences on coupling during hospitalization. We observed a significant Time and Condition interaction ($F_{(1,109.7)}=5.99$, $P=.016$; Figure 1 and Supplemental Table 3) with post-hoc analyses demonstrating significantly greater coupling during task versus rest conditions at visit 1 ($(t_{(109.7)})=6.19$, $P<.001$) and visit 2 ($(t_{(109.7)})=2.65$, $P=.045$). During hospitalization, a significant decrease in coupling during task performance occurred across individuals from visit 1 to visit 2 ($(t_{(109.7)})=-4.03$, $P<.001$). The bimodal distribution and heterogeneity depicted during the task condition at visit 1 (Figure 1), which was collapsed across Extremity, warranted additional analysis as performed below.

Heightened Coupling During Affected Extremity Task Performance

We performed a third mixed-effects linear model that accounted for Group, Extremity, and Time yielding a significant 3-way interaction ($F_{(1,70.4)}=38.33$, $P<.001$; Figure 2 and Supplemental Table 4). Post-hoc analyses showed significantly greater coupling in individuals with

Table 1. Participant Demographics and Clinical Measures.

Descriptor	n	Mean (SD) or median [IQR]	Range
Sex (female/male)			
Female	14	—	—
Male	16	—	—
Race, ethnicity			
Black, non-Hispanic	6	—	—
White, non-Hispanic	24	—	—
Age (years)		67.0 (9.8)	51-85
Lesioned hemisphere			
Left	12	—	—
Right	18	—	—
Stroke type			
Hemorrhagic	2	—	—
Ischemic	28	—	—
Days post-stroke to enrollment		10.4 (3.5)	5-18
Days between study visits	29	11.9 (6.5)	3-28
NIHSS (max = 42)		3.0 [1.0-6.2]	0-17
Lesion volume (cc)		19.9 (35.9)	0.08-155.7
BG lesion overlap (%)	29	8.3 (10.5)	0-38.4
ATR lesion overlap (%)	29	7.5 (11.5)	0-41.4
CST lesion overlap (%)	29	8.9 (6.6)	0.02-22.2
UEFM (max = 66)			
Visit 1		40.9 (25.1)	2-66
Visit 2	29	46.8 (23.6)	4-66
Change	29	6.4 (9.6)	-7-41
ARAT (max = 57)			
Visit 1		33.0 (23.7)	0-57
Visit 2	28	37.1 (24.1)	0-57
Change	28	5.3 (9.2)	-2-37
MoCA (max = 30)			
Visit 1	28	22.3 (4.2)	14-29
Visit 2	29	23.9 (5.4)	11-30
Change	28	1.6 (3.2)	-7-6
Affected extremity grip (kg)			
Visit 1	28	11.5 (11.9)	0-36.7
Visit 2	29	14.1 (12.2)	0-37.3
Change	28	2.49 (4.5)	-6.8-13.3
Less-affected extremity grip (kg)			
Visit 1	28	27.3 (11.6)	8.7-56.7
Visit 2	29	29.0 (11.2)	9.3-55.3
Change	28	2.2 (5.2)	-6.0-17.3

Note. Values presented as mean (standard deviation, SD) or median [interquartile range, IQR]. Number of participants is $n=30$ unless otherwise noted. Abbreviations: IRF, inpatient rehabilitation facility; NIHSS, National Institutes of Health Stroke Scale; cc, cubic centimeters; BG, basal ganglia; ATR, anterior thalamic radiation; CST, corticospinal tract; UEFM, Upper Extremity Fugl-Meyer; ARAT, Action Research Arm Test; MoCA, Montreal Cognitive Assessment.

stroke during task performance from the affected extremity throughout hospitalization (Visit 1: $t_{(70,4)}=21.53$, $P<.001$; Visit 2: $t_{(70,4)}=7.86$, $P<.001$). Coupling during task performance with the affected extremity was also significantly lower at visit 2 as compared with visit 1 ($t_{(70,4)}=15.13$, $P<0.001$). Similar coupling differences

across Time were not observed for the less-affected extremity task performance ($t_{(70,4)}=1.13$, $P=.948$).

Additional post-hoc testing from the above model indicated significantly greater coupling during the task condition from the stroke-affected extremity versus dominant (Visit 1: $t_{(70,4)}=13.49$, $P<.001$; Visit 2: $t_{(70,4)}=3.38$,

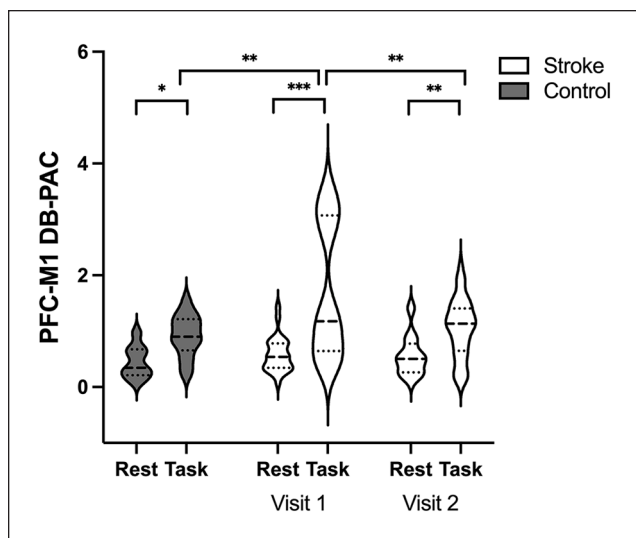


Figure 1. Enhancement of PFC-M1 DB-PAC during task performance. Participants with stroke and controls demonstrated greater DB-PAC during the task (collapsed across extremity) versus rest condition. * $P < .05$. ** $P < .01$. *** $P < .001$.

$P = .025$) and non-dominant (Visit 1: $t_{(70,4)} = 13.91, P < .001$; Visit 2: $t_{(70,4)} = -3.48, P = .018$) extremities from control participants (Figure 2).

To further characterize observed DB-PAC, we investigated the delta PFC phase-dependency of M1 beta amplitude across recovery (Figure 3). This analysis revealed that M1 beta amplitude was strongest around the peak of the PFC delta phase during affected extremity task performance at visit 1 (Figure 3B) and shifted toward the rising phase at visit 2 (Figure 3C) thereby resembling controls (Figure 3A).

Control Assessment of EEG Power and Within MI-Coupling

To confirm that modulations in EEG power did not account for PFC-M1 DB-PAC in individuals with stroke, we repeated the above-described 3-factor linear model replacing PAC with delta power in electrodes overlying PFC (PFC_{delta}) and beta power in electrodes overlying contralateral M1 ($M1_{\text{beta}}$). There was no significant Group, Extremity, and Time interaction across participants (PFC_{delta} : $F_{(1,70,4)} = 1.01, P = .326$; $M1_{\text{beta}}$: $F_{(1,70,4)} = 0.01, P = .923$).

An FFT performed across the scalp confirms the presence of delta and beta oscillatory activity across the scalp and within M1 (Supplemental Figure 2). The linear model was also repeated accounting for DB-PAC within M1 to further isolate the neural activity within M1 independent of other cortical involvement. This model showed no significant Group, Extremity, and Time interaction ($F_{(1,70,4)} = 0.054, P = .816$).

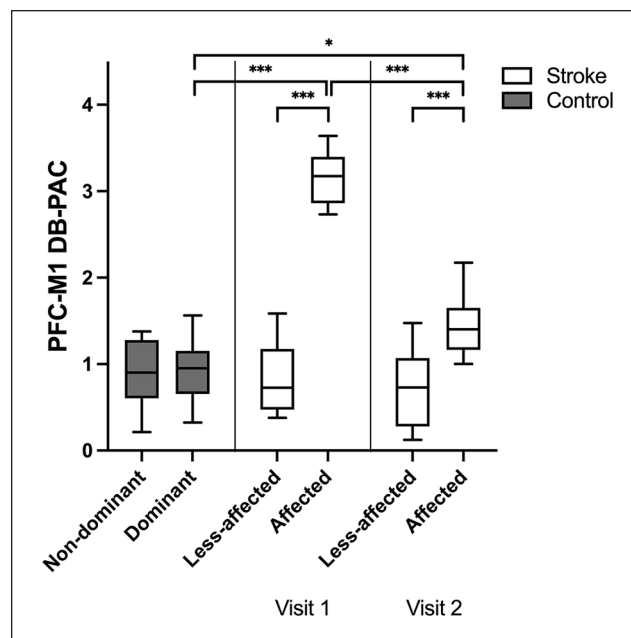


Figure 2. Enhanced ipsilesional PFC-M1 DB-PAC during task performance with the affected extremity. Individuals with stroke demonstrated significantly greater coupling during task performance with their affected versus less-affected extremity at visits 1 and 2 despite a significant decrease in coupling during affected extremity performance between visits. * $P < .05$. ** $P < .01$. *** $P < .001$.

Localization of Coupling Toward Ipsilesional M1

Overall, the clustering analysis revealed a wide distribution of coupling across the cortical surface during affected extremity task performance at visit 1 with some localization around ipsilesional M1 (Figure 4A). The cluster analysis also indicated that coupling in electrodes most closely corresponded to C3 (associated with ipsilesional M1) were significantly associated with a Group and Time interaction (Figure 4B).

Coupling Across the PFC-PMC-M1 Pathway

To examine coupling along the PFC-PMC-M1 pathway, we performed a series of partial correlations involving DB-PAC between PFC-PMC, PFC-M1, and PMC-M1. At visit 1, PFC-M1 coupling was positively associated with PFC-PMC coupling during affected extremity task performance ($r = .82, P < .001$). This relationship persisted after accounting for PMC-M1 coupling ($r_{\text{partial}} = .82, P < .001$) as coupling associations involving PFC-M1 and PMC-M1 were not observed ($r_{\text{partial}} = -.01, P = .983$). At visit 2, PFC-M1 coupling was again positively associated with PFC-PMC coupling ($r = .60, P = .008$) and remained significant after accounting for PMC-M1 coupling ($r_{\text{partial}} = .65, P = .005$). Greater PFC-M1 coupling was now also

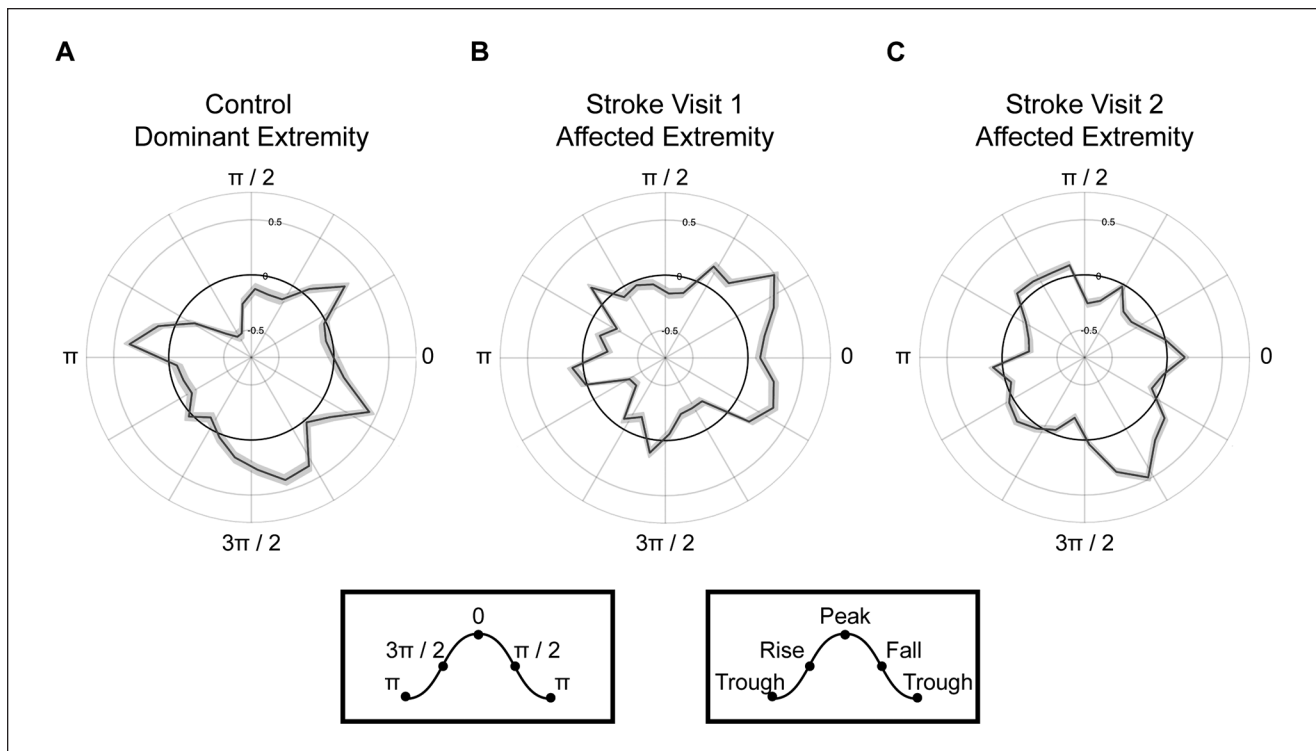


Figure 3. Stroke shifts M1 beta amplitude to the rise of PFC delta phase. Rose plots of PFC delta phase coupled to M1 beta amplitude (black line) in (A) control participants during task performance with the dominant extremity, (B) individuals with stroke during task performance with the affected extremity at visit 1 and visit 2 (C). A shift in phase-dependency from the peak of the delta PFC phase to the rise of the delta PFC phase occurred between visits 1 and 2. Grey shading around the black line indicates standard error. Peak and trough values in radians provide additional orientation.

associated with greater PMC-M1 coupling ($r_{\text{partial}} = .49$, $P = .047$, Supplemental Figure 3).

Coupling, Neural Injury, and Motor Status

Larger lesion volume was associated with greater PFC-M1 coupling ($\rho = .60$, $P = .023$), while greater lesion overlap to ATR was negatively associated with coupling ($\rho = -.61$, $P = .025$; Supplemental Figure 4). Associations between coupling and lesion overlap injury to BG ($\rho = .25$, $P = .588$) and CST ($\rho = -.51$, $P = .089$) were not significant. These findings informed the construction of a preliminary conceptual model of PFC-M1 DB-PAC (Figure 5). Greater coupling at baseline was associated with better motor status around IRF admission (UEFM: $\rho = .59$, $P = .026$; ARAT: $\rho = .55$, $P = .041$; Supplemental Figure 5) and discharge (UEFM: $\rho = 0.39$, $P = .056$; ARAT: $\rho = .44$, $P = .026$). Baseline coupling also positively correlated with motor recovery during IRF stay (ARAT Change_{Realized}: $\rho = .46$, $P = .048$). Participants demonstrated a significant increase in affected extremity grip strength during IRF hospitalization ($t = 2.73$, $P = .011$; Supplemental Figure 6). Prefrontomotor coupling at visit 1 did not correlate with change in affected extremity maximal grip strength during

IRF hospitalization ($\rho = -.04$, $P = .884$). No change in less-affected extremity grip strength occurred during IRF hospitalization ($t = 1.98$, $P = .058$).

Discussion

In the current study, we computed PFC-M1 DB-PAC in persons with stroke during their IRF stay to determine the utility of prefrontomotor coupling as a potential motor recovery biomarker. We found that individuals with stroke demonstrated greater prefrontomotor coupling compared to controls during task performance with the affected extremity near IRF admission and discharge. Greater coupling at admission was also acutely related to injury magnitude and associated with motor status and recovery.

On several fronts, this work represents both a continuation and departure from past connectivity studies in stroke. This study focused on delta and beta oscillatory activity based on prior work relating neural injury and motor recovery to these particular frequency bands.^{5,20} Previous PAC examination in stroke has focused mainly on theta (4-7 Hz), alpha (8-12 Hz), and beta (13-29 Hz) phase coupling with gamma (65-100 Hz) amplitude between M1 regions.¹² While functional connectivity between ipsi- and

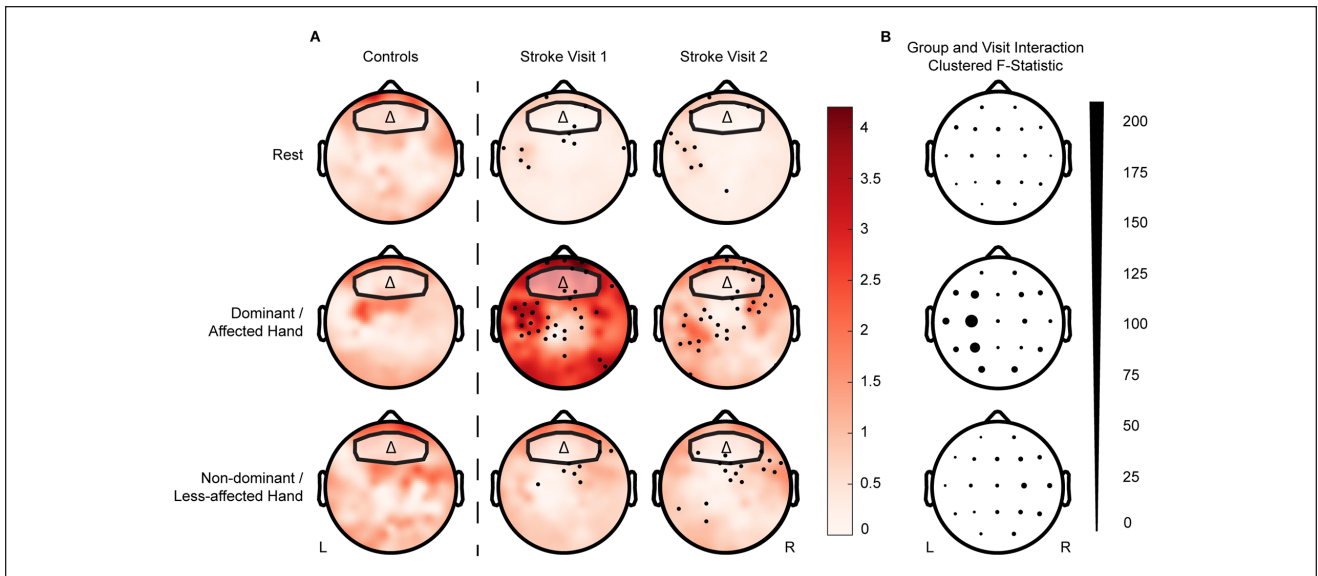


Figure 4. Cluster analysis of prefrontal delta and scalp beta coupling. (A) Topographical plots demonstrating coupling between delta phase of electrodes overlying PFC (outlined box) and scalp beta amplitude. Electrodes showing a significant Group effect (Bonferroni-corrected $P=.00026$) are plotted for each visit. Darker red color reflects greater coupling. (B) Graphical presentation of the clustered F-statistic for the Group and Time interaction across electrodes triangulated to 10 to 20 neighbors presented. Larger electrodes reflect a greater interaction. Coupling is greatest in the ipsilesional hemisphere during affected extremity task performance (B, middle). During non-dominant and less-affected extremity performance, the interaction is greater in clustered electrodes overlying the contralesional hemisphere (B, bottom). L indicates the left or ipsilesional hemisphere, and R indicates the right or contralesional hemisphere.

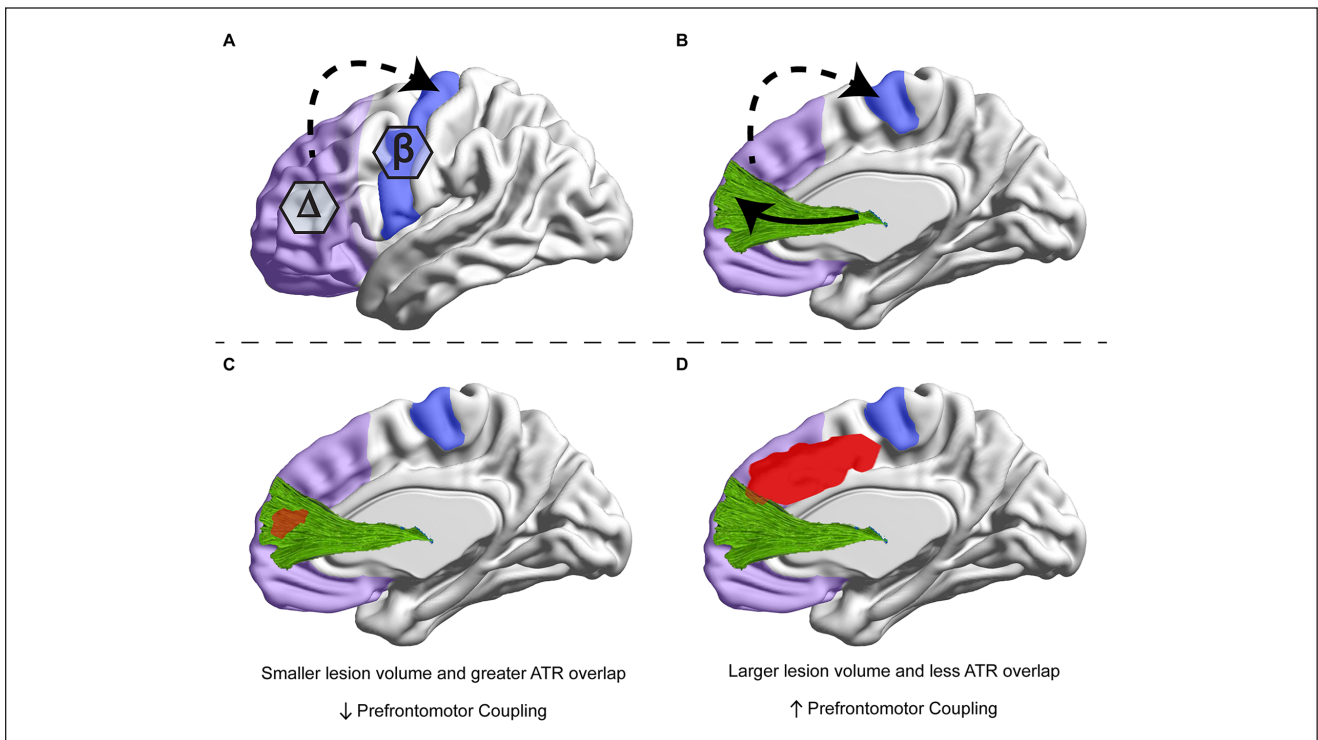


Figure 5. Proposed conceptual model of a PFC-MI DB-PAC network. Delta oscillatory activity from prefrontal cortex (PFC, purple) modulates beta oscillatory activity from nearby primary motor cortex (MI, blue) through (A) functional connections (dotted arrow) and (B) structural connections (solid arrow) via white matter fiber tracts such as the anterior thalamic radiation (ATR, green). (C) Smaller lesion volume and greater ATR overlap injury (red) are associated with less coupling. (D) Larger lesion volume and less ATR overlap injury are associated with greater coupling.

contralateral M1 regions has repeatedly shown relevance in post-stroke motor recovery,⁴³ contributions from other cortical regions merit consideration. Our focus on cross-frequency coupling between electrodes overlying PFC and M1 regions, combined with preliminary examination of PFC and M1 coupling with PMC, represents a novel coupling approach in stroke. The involvement of PFC in coupling analyses, in comparison to bilateral M1 regions, also aligns with the notion of post-stroke rehabilitation as a biopsychosocial process involving motor re-learning; whereby, cognitive functioning and person-centered factors such as motivation and self-efficacy impact rehabilitation and re-learning outcomes.⁴⁴

The linear mixed models performed in this work to discern within- and between-group differences generated several important findings. As hypothesized, initial modeling revealed greater coupling during task performance as compared to rest, which may be attributable to greater cognitive demand (ie, PFC involvement) in the former condition. Importantly, group differences in coupling emerged during the task condition and were specific to the affected extremity for those with stroke as no between- or within-group differences in coupling during *less-affected* extremity performance were observed. Though individuals with stroke demonstrated a reduction in coupling during affected extremity performance over the course of their IRF stay, coupling remained elevated at around the time of IRF discharge relative to controls. This likely reflects the ongoing and incomplete nature of early post-stroke motor recovery.⁴⁵

Relatedly, an exploratory investigation of coupling along the PFC-PMC-M1 pathway demonstrated the involvement of secondary motor regions (PMC). Our finding of PFC-M1 coupling positively related to PMC-M1 coupling at visit 2, but not at visit 1, partially supports our hypothesis that coupling between PFC and M1 occurs through PMC. The changes in coupling between PFC-M1, PFC-PMC, and PMC-M1 from visit 1 to visit 2 may reflect a greater reliance on executive control from PFC in motor control during earlier recovery stages. Our overall finding of decreased DB-PAC coupling between PFC and M1 over time (Figure 2) may also therefore represent a greater influence of oscillatory activity from PMC on M1 that emerges during recovery.

Positive associations between coupling during affected extremity task performance and motor status (UEFM and ARAT scores) at visits 1 and 2 and motor recovery (ARAT Change_{Realized}) combined with the cluster analysis findings (Figure 4B) suggest that increased cortical activity arising from the ipsilesional hemisphere contributes to better motor outcomes by the start and end of inpatient rehabilitation. This finding aligns with prior meta-analyses reporting more favorable motor recovery outcomes with more localized ipsilesional motor cortical activity.^{46,47} Therefore, PFC-M1 DB-PAC may represent an adaptive neuroplasticity

mechanism particularly beneficial during earlier post-stroke recovery timeframes when the execution of goal-directed movement may present greater attentional demands and reliance on PFC.

Apart from compensatory or adaptive neuroplasticity mechanisms, the temporal dynamics of DB-PAC observed in this work may relate to motor control, including movement planning, preparation, and execution phases. Linking the temporal dynamics of DB-PAC to motor control is difficult as our understanding of the functional relevance of delta and beta oscillatory activity continues to evolve. For instance, beta oscillatory activity increases during motor planning and decreases with movement execution,⁴⁸ suggesting its utility in preparing and holding the motor system in a “ready state” prior to the initiation of movement.⁴⁹ Consequently, beta oscillatory activity *during* movement has been associated with pathological movement entailing akinesia and/or hypokinesia.⁵⁰ This contrasts with the involvement of delta-high gamma coupling during the execution of complex movements in humans⁵¹ and motor control improvement (ie, dexterity) following the restoration of low-frequency activity with alternating current stimulation in primates following stroke.⁵² Our findings of elevated DB-PAC during task performance implies a more nuanced role for coupling in motor control post-stroke whereby DB-PAC serves a regulatory-like function during the sustainment phase of movement of our grip task. During this time, contributions from PFC extend beyond movement preparation and initiation to now encompass continuous communication with M1 so that participants’ generated force output matches and maintains the force associated with the visual target. This interaction may be particularly beneficial post-stroke amidst disruptions in neural network connectivity. Our findings indicate that PFC exerts a stronger regulatory influence on PMC and M1 to achieve the desired motor output at visit 1 versus 2. We therefore propose that elevated DB-PAC observed exclusively during task versus rest conditions in this study, represents top-down regulation of motor execution that is augmented during early post-stroke recovery. Comparing and/or contrasting the temporal dynamics of DB-PAC during motor recruitment and sustainment phases is a necessary next step.

When determining the effect of stroke-related injury on coupling, we included both general (lesion volume) and coupling-specific (ATR, CST, and BG overlap injury) measurements. Interestingly, we observed divergent findings between injury and PFC-M1 DB-PAC near IRF admission. Greater coupling was associated with *larger* lesion volume and *smaller* lesion overlap to ATR. The first finding involving lesion volume relates to prior work showing positive associations between enhanced delta coherence involving ipsilesional M1 and larger infarct volume.²⁰ Enhanced delta activity arising as a function of lesion extent may have thus contributed to increased DB-PAC in this work. Because few participants sustained direct damage to the PFC region and

were subsequently removed for these correlational analyses, it is possible that enhanced delta activity in electrodes overlying the PFC region may have occurred through mechanisms consistent with diaschisis. The second finding involving ATR injury resonates with past work demonstrating altered resting-state functional connectivity with white matter injury following stroke.⁵³ A notable feature of this past work was the focus on white matter integrity of the CST in upstream sensorimotor functional connectivity. In our work, associations between CST injury and coupling were not significant, suggesting that PFC-M1 DB-PAC may not rely on the structural integrity of this tract. Our results indicated that injury to ATR, a white matter tract connecting thalamus (anterior and midline nuclei) with the frontal lobe, which is frequently used to anatomically define PFC,³¹ may be a key PFC-M1 DB-PAC substrate. This finding is bolstered by prior rodent work showing the mediation of beta oscillatory activity in PFC by the thalamic nucleus reuniens, which is part of the midline thalamic nuclei group³³ closely aligned with ATR. Further, work in humans has shown enhanced activation of the anterior thalamus (also closely aligned with ATR) during complex task performance.³⁰ Lastly, we observed no association between coupling and BG overlap injury. This may suggest that prefrontal control or gating of M1 activity occurs through structural white matter tracts and/or branches of these tracts rather than through individual subcortical nuclei comprising the CBGTC loop.

This study presents several strengths, including the collection of neuroimaging, behavioral, and neurophysiological assessments often acquired at 2 distinct timepoints during post-stroke rehabilitation. The heterogeneity of our stroke cohort promotes the generalizability of our findings; however, the examination of more homogenous subgroups (eg, moderate-severe vs mild motor impairment or cortical vs subcortical lesion involvement) in future work may determine if distinct patterns or profiles of PFC-M1 DB-PAC exist in specific subgroups. There are a few limitations in this work to acknowledge. Due to the exploratory nature of this work, we did not control for potential confounders such as baseline motor impairment, age, time-post stroke, and length of IRF stay. Also, compared to other PAC studies that involved tasks of spatial attention, object abstraction, and decision making,^{10,13,15} the precision grip task included in this study may not have possessed the same degree of cognitive demand, which may have influenced prefrontal gating of motor activity. We also note the limitations with our injury measurement involving lesion overlap with white matter tracts, which may not capture subtle characteristics of tract integrity as compared to more sensitive diffusion-based measures.⁵⁴ Finally, we recognize that the sensitivity of the dynamometer device and physical demands of the grip task prohibited participation from a few individuals with severe hemiparesis.

Conclusions

The early post-stroke recovery timeframe represents a period of enriched plasticity.⁵⁵ Measures that capture these neuroplasticity mechanisms of post-stroke recovery and re-learning have the potential to advance stroke rehabilitation research by providing novel treatment strategies. In line with precision medicine-based approaches that often entail treatment delivery to gene- and cell-specific targets, the frequency- and region-specific neurocircuitry featured in this work may offer additional treatment targets to non-invasive brain stimulation application. Likewise, the translation of non-invasive brain stimulation protocols to clinical practice in stroke requires a comprehensive understanding of the mechanisms behind these treatments to ensure for more personalized delivery.⁵⁶ The measurement and examination of PAC, along with shifts in phase dependency across post-stroke recovery, may provide crucial mechanistic understanding to propel translation. Lastly, stroke often results in multiple impairments spanning multiple domains (eg, motor, cognitive, language, and visuospatial). Recognizing the potential overlap or interaction between impairments is critical yet not fully realized, especially in the development of post-stroke motor recovery biomarkers used to predict recovery outcomes. The measurement and assessment of PAC between PFC and M1 in this work thus represents an important methodological pathway toward advancing our understanding of post-stroke recovery wherein the consideration of cross-frequency intercortical interactions affords a more holistic perspective to recovery.

Acknowledgments

We thank Drs. John M. Baratta, MD, MBA and Kelly Fletcher, PT, DPT for their assistance with participant enrollment and recruitment.

Author Contributions

Jasper I. Mark: Data curation; Formal analysis; Visualization; Writing—original draft. Justin Riddle: Conceptualization; Formal analysis; Methodology; Resources; Supervision; Visualization; Writing—review & editing. Rachana Gangwani: Data curation; Investigation; Writing—review & editing. Benjamin Huang: Validation; Writing—review & editing. Flavio Frohlich: Resources; Supervision; Visualization; Writing—review & editing. Jessica M. Cassidy: Conceptualization; Data curation; Funding acquisition; Investigation; Methodology; Project administration; Supervision; Writing—original draft.

Declaration of Conflicting Interests


The author(s) declared the following potential conflicts of interest with respect to the research, authorship, and/or publication of this article: JM reports stock holdings in Impulse Wellness LLC. FF is the lead inventory of IP filed on the topics of non-invasive brain stimulation by UNC. FF has received honoraria from the

following entities in the last 12 months: Electromedical Products International, Academic Press, and Insel Spital. All other authors have no competing interests to disclose.

Funding

The author(s) disclosed receipt of the following financial support for the research, authorship, and/or publication of this article: This research received funding from an NIH R00HD091375 (JMC) and NIH K99MH126161 (JR).

ORCID iD

Jessica M. Cassidy  <https://orcid.org/0000-0003-3469-0399>

References

- Cramer SC. Repairing the human brain after stroke: I. Mechanisms of spontaneous recovery. *Ann Neurol*. 2008;63(3):272-287.
- Cassidy JM, Tran G, Quinlan EB, Cramer SC. Neuroimaging identifies patients most likely to respond to a restorative stroke therapy. *Stroke*. 2018;49(2):433-438.
- Tedesco Triccas L, Meyer S, Mantini D, et al. A systematic review investigating the relationship of electroencephalography and magnetoencephalography measurements with sensorimotor upper limb impairments after stroke. *J Neurosci Methods*. 2019;311:318-330.
- Kawano T, Hattori N, Uno Y, et al. Association between aphasia severity and brain network alterations after stroke assessed using the electroencephalographic phase synchrony index. *Sci Rep*. 2021;11(1):12469.
- Cassidy JM, Wodeyar A, Srinivasan R, Cramer SC. Coherent neural oscillations inform early stroke motor recovery. *Hum Brain Mapp*. 2021;42:5636-5647.
- Wu J, Quinlan EB, Dodakian L, et al. Connectivity measures are robust biomarkers of cortical function and plasticity after stroke. *Brain*. 2015;138(8):2359-2369.
- Meder D, Siebner HR. Spectral signatures of neurodegenerative diseases: how to decipher them? *Brain*. 2018;141(8):2241-2244.
- Liu X, Pu Y, Wu D, Zhang Z, Hu X, Liu L. Cross-frequency coupling between cerebral blood flow velocity and EEG in ischemic stroke patients with large vessel occlusion. *Front Neurol*. 2019;10:194.
- Canolty RT, Edwards E, Dalal SS, et al. High gamma power is phase-locked to theta oscillations in human neocortex. *Science*. 2006;313(5793):1626-1628.
- Riddle J, McFerren A, Frohlich F. Causal role of cross-frequency coupling in distinct components of cognitive control. *Prog Neurobiol*. 2021;202:102033.
- Cohen MX. Multivariate cross-frequency coupling via generalized eigendecomposition. *Elife*. 2017;6:e21792.
- Rustamov N, Humphries J, Carter A, Leuthardt EC. Theta-gamma coupling as a cortical biomarker of brain-computer interface-mediated motor recovery in chronic stroke. *Brain Commun*. 2022;4(3):fcac136.
- Riddle J, Alexander ML, Schiller CE, Rubinow DR, Frohlich F. Reward-based decision-making engages distinct modes of cross-frequency coupling. *Cereb Cortex*. 2022;32(10):2079-2094.
- Cohen MX, Elger CE, Fell J. Oscillatory activity and phase-amplitude coupling in the human medial frontal cortex during decision making. *J Cogn Neurosci*. 2009;21(2):390-402.
- Rahnev D, Nee DE, Riddle J, Larson AS, D'Esposito M. Causal evidence for frontal cortex organization for perceptual decision making. *Proc Natl Acad Sci USA*. 2016;113(21):6059-6064.
- Quinlan EB, Cramer SC. Biomarkers and predictors of restorative therapy effects after stroke. *Curr Neurol Neurosci Rep*. 2013;13(2):239.
- Westlake K, Nagarajan S. Functional connectivity in relation to motor performance and recovery after stroke. *Front Syst Neurosci*. 2011;5:8.
- Davare M, Rothwell JC, Lemon RN. Causal connectivity between the human anterior intraparietal area and premotor cortex during grasp. *Curr Biol*. 2010;20(2):176-181.
- Nashef A, Mitelman R, Harel R, Joshua M, Prut Y. Area-specific thalamocortical synchronization underlies the transition from motor planning to execution. *Proc Natl Acad Sci USA*. 2021;118(6):e2012658118.
- Cassidy JM, Wodeyar A, Wu J, et al. Low-frequency oscillations are a biomarker of injury and recovery after stroke. *Stroke*. 2020;51(5):1442-1450.
- Wu J, Srinivasan R, Burke Quinlan E, Solodkin A, Small SL, Cramer SC. Utility of EEG measures of brain function in patients with acute stroke. *J Neurophysiol*. 2016;115(5):2399-2405.
- Garey LJ. *Brodman's Localisation in the Cerebral Cortex*. World Scientific; 1999.
- Rizzolatti G, Fogassi L, Gallese V. Motor and cognitive functions of the ventral premotor cortex. *Curr Opin Neurobiol*. 2002;12(2):149-154.
- Abe M, Hanakawa T. Functional coupling underlying motor and cognitive functions of the dorsal premotor cortex. *Behav Brain Res*. 2009;198(1):13-23.
- Matelli M, Govoni P, Galletti C, Kutz DF, Luppino G. Superior area 6 afferents from the superior parietal lobule in the macaque monkey. *J Comp Neurol*. 1998;402(3):327-352.
- Johnson PB, Ferraina S, Bianchi L, Caminiti R. Cortical networks for visual reaching: physiological and anatomical organization of frontal and parietal lobe arm regions. *Cereb Cortex*. 1996;6(2):102-119.
- Davare M, Andres M, Cosnard G, Thonnard JL, Olivier E. Dissociating the role of ventral and dorsal premotor cortex in precision grasping. *J Neurosci*. 2006;26(8):2260-2268.
- Vesia M, Culham JC, Jegatheeswaran G, et al. Functional interaction between human dorsal premotor cortex and the ipsilateral primary motor cortex for grasp plans: a dual-site TMS study. *Neuroreport*. 2018;29(16):1355-1359.
- Logiaco L, Abbott LF, Escola S. Thalamic control of cortical dynamics in a model of flexible motor sequencing. *Cell Rep*. 2021;35(9):109090.
- Lehéricy S, Bardin E, Tremblay L, et al. Motor control in basal ganglia circuits using fMRI and brain atlas approaches. *Cereb Cortex*. 2005;16(2):149-161.

31. George K, Das J. *Neuroanatomy, Thalamocortical Radiations*. StatPearls Publishing; 2023.
32. Ganguly K, Khanna P, Morecraft RJ, Lin DJ. Modulation of neural co-firing to enhance network transmission and improve motor function after stroke. *Neuron*. 2022;110(15):2363-2385.
33. Jayachandran M, Viena TD, Garcia A, et al. Nucleus reuniens transiently synchronizes memory networks at beta frequencies. *Nat Commun*. 2023;14(1):4326.
34. Lin DJ, Cloutier AM, Erler KS, et al. Corticospinal tract injury estimated from acute stroke imaging predicts upper extremity motor recovery after stroke. *Stroke*. 2019;50(12):3569-3577.
35. Mark JI, Ryan H, Fabian K, DeMarco K, Lewek MD, Cassidy JM. Aerobic exercise and action observation priming modulate functional connectivity. *PLoS One*. 2023;18(4):e0283975.
36. Delorme A, Sejnowski T, Makeig S. Enhanced detection of artifacts in EEG data using higher-order statistics and independent component analysis. *Neuroimage*. 2007;34(4):1443-1449.
37. Badre D, D'Esposito M. Functional magnetic resonance imaging evidence for a hierarchical organization of the prefrontal cortex. *J Cogn Neurosci*. 2007;19(12):2082-2099.
38. McFerren A, Riddle J, Walker C, Buse JB, Frohlich F. Causal role of frontal-midline theta in cognitive effort: a pilot study. *J Neurophysiol*. 2021;126(4):1221-1233.
39. Hülsemann MJ, Naumann E, Rasch B. Quantification of phase-amplitude coupling in neuronal oscillations: comparison of phase-locking value, mean vector length, modulation index, and generalized-linear-modeling-cross-frequency-coupling. *Front Neurosci*. 2019;13:573.
40. Quinlan EB, Dodakian L, See J, et al. Neural function, injury, and stroke subtype predict treatment gains after stroke. *Ann Neurol*. 2015;77(1):132-145.
41. Rolls ET, Huang C-C, Lin C-P, Feng J, Joliot M. Automated anatomical labelling atlas 3. *Neuroimage*. 2020;206:116189.
42. Oishi K, Crain BJ. *MRI Atlas of Human White Matter*. New York Academic Press; 2010.
43. Cassidy JM, Mark JI, Cramer SC. Functional connectivity drives stroke recovery: shifting the paradigm from correlation to causation. *Brain*. 2022;145(4):1211-1228.
44. Gangwani R, Cain A, Collins A, Cassidy JM. Leveraging factors of self-efficacy and motivation to optimize stroke recovery. *Front Neurol*. 2022;13:823202.
45. Hendricks HT, van Limbeek J, Geurts AC, Zwartz MJ. Motor recovery after stroke: a systematic review of the literature. *Arch Phys Med Rehabil*. 2002;83(11):1629-1637.
46. Favre I, Zeffiro TA, Detante O, Krainik A, Hommel M, Jaillard A. Upper limb recovery after stroke is associated with ipsilesional primary motor cortical activity: a meta-analysis. *Stroke*. 2014;45(4):1077-1083.
47. Rehme AK, Eickhoff SB, Rottschy C, Fink GR, Grefkes C. Activation likelihood estimation meta-analysis of motor-related neural activity after stroke. *Neuroimage*. 2012;59(3):2771-2782.
48. Pfurtscheller G, Da Silva FL. Event-related EEG/MEG synchronization and desynchronization: basic principles. *Clin Neurophysiol*. 1999;110(11):1842-1857.
49. Saleh M, Reimer J, Penn R, Ojakangas CL, Hatsopoulos NG. Fast and slow oscillations in human primary motor cortex predict oncoming behaviorally relevant cues. *Neuron*. 2010;65(4):461-471.
50. Lofredi R, Neumann WJ, Brücke C, et al. Pallidal beta bursts in Parkinson's disease and dystonia. *Mov Disord*. 2019;34(3):420-424.
51. Natraj N, Silversmith DB, Chang EF, Ganguly K. Compartmentalized dynamics within a common multi-area mesoscale manifold represent a repertoire of human hand movements. *Neuron*. 2022;110(1):154-174.e112.
52. Khanna P, Totten D, Novik L, Roberts J, Morecraft RJ, Ganguly K. Low-frequency stimulation enhances ensemble co-firing and dexterity after stroke. *Cell*. 2021;184(4):912-930.e920.
53. Hordacre B, Goldsworthy MR, Welsby E, Graetz L, Ballinger S, Hillier S. Resting state functional connectivity is associated with motor pathway integrity and upper-limb behavior in chronic stroke. *Neurorehabil Neural Repair*. 2020;34(6):547-557.
54. Assaf Y, Pasternak O. Diffusion Tensor Imaging (DTI)-based white matter mapping in brain research: a review. *J Mol Neurosci*. 2008;34(1):51-61.
55. Cassidy JM, Cramer SC. Spontaneous and therapeutic-induced mechanisms of functional recovery after stroke. *Transl Stroke Res*. 2017;8(1):33-46.
56. Edwards JD, Dominguez-Vargas AU, Rosso C, et al. A translational roadmap for transcranial magnetic and direct current stimulation in stroke rehabilitation: consensus-based core recommendations from the third stroke recovery and rehabilitation roundtable. *Neurorehabil Neural Repair*. 2024;38(1):19-29.